Study of Type-A Zeolites. Part 2: Effect of Dehydration on the Effective Aperture Dimension

Avraham Saig, Yacov Finkelstein, Albert Danon, and Jacob E. Koresh*

Chemistry Division, Nuclear Research Center of the Negev (NRCN), Beer-Sheva 84190, Israel

Received: May 25, 2003; In Final Form: September 25, 2003

A new insight into the role played by water molecules in the crystalline framework of type-A zeolites is demonstrated. The effect of dehydration on the effective free aperture dimension, D_f, is studied by utilizing temperature-programmed decapsulation of He and Ne. The interplay between the various known mechanisms governing D_f is directly sensed by the decapsulation behavior of differently sized inert atoms. The results are qualitatively interpreted using pure dimensional considerations, revealing the occurrence of a strict relation between the content of water molecules and the redistribution of zeolitic cations in determining D_f. Water content is shown to have a strong effect on the blocking state of the O_8 and O_6 zeolitic windows, which in turn, governs gas accessibility to the α and β cages. It is proposed that D_f is regulated via a subtle balance between two coupled principal mechanisms. One involves direct lattice adjustments, where two opposite sub-mechanisms seem to play competitive roles. Removal of water molecules by simultaneous heating and pumping enlarges D_f, while hydroxyl groups elimination from within the zeolitic channels results in their partial collapse, thus reducing D_f. The second mechanism involves the regulation of aperture blocking via relocations of the counterions initiated by increasing vacancies due to removal of water molecules. While dehydration continuously contracts the O_6 apertures, a two-stage effect is observed for the wider O_8 windows. Upon dehydration at large water contents, O_8 apertures are reduced; then, beyond a critical extent of dehydration, the net effect is reversed, widening the O_8 windows.

Introduction

The occurrence of ambient pressure encapsulation of He and Ne in type-A zeolites, its critical sorption conditions, and the mechanism by which it is governed, were established in Part 1.[1] Counterions relocations and lattice adjustments were shown to interplay in the determination of the effective apertures dimension in those zeolites. All of the above were established for the case of completely dehydrated A-zeolite samples. An interesting question raised during the above study concerns the nature of the effect that water content has on encapsulation, and is dehydration a useful tool that may be utilized for probing the roles taken by the various mechanisms governing encapsulation, as well as their intra-relationships, in determining the effective dimension of zeolitic apertures.

Upon complete dehydration, many zeolites undergo irreversible structural changes up to a total structural collapse.[2,3] In most cases these constructions may be dehydrated to some degree without major alteration of their crystalline structure. In zeolites that undergo continuous and reversible dehydration, there is no substantial change in the topology of the framework structure. Type-A zeolites are known to undergo a continuous water loss ($\leq$ 23 wt %) with increasing temperature between room temperature (RT) to about 300 °C without any resultant structural variations. The role of water content is of a fundamental importance for understanding the factors governing the encapsulation mechanism. It was only rarely studied in relation to its effect on the mobility and relocations of the neutralizing counterions. These early works mostly utilized various adsorbed phases of dipolar and quadrupolar species. The effect of their interactions with the anionic lattice and field gradients at the cations sites, on the electrical conductivity of the zeolite was studied. In such recent study,[4] the measured data could only qualitatively indicate the occurrence of a multi stage dehydration process. Water molecules are frequently associates with the zeolitic cations,[5,6] which in turn play a major role in determining the blocking status of the zeolitic apertures. Zeolite frameworks usually provide more than one kind of site for the exchangeable cations. By occupying available sites among the anionic framework, the cations distribute themselves in order to electrically balance it and minimize the free energy of the system. For a given temperature and cationic species the distribution equilibrium is a function of dehydration of the zeolite,[5,6] and this in turn is expected to affect the encapsulation process.

In the present study, the effect of water content on the process of *encapsulation* is *directly* studied by measuring the behavior of decapsulation versus zeolite grade (3, 4, and 5A), temperature ($77\ K > T > 673\ K$) and size of encapsulated gas (He and Ne). By using He and Ne as inert, nondipolar, nonquadrupolar atomic probes, most physical interactions are eliminated, and only net geometrical effects are purely sensed. As a result, the role of water content in governing the blocking states of the zeolitic apertures is extracted, providing new information on the interplay taken between the various mechanisms governing zeolitic encapsulation.

Experimental Section

The experimental details of the temperature-programmed decapsulation (TPD_c) measurements were previously discussed and described.[1,8] In the present study, the effect of dehydration on He and Ne encapsulation was studied for the three family

* Corresponding author. E-mail: jacobk@nrcn.org.il.

10.1021/jp035447j CCC: $25.00
Published on Web 11/07/2003

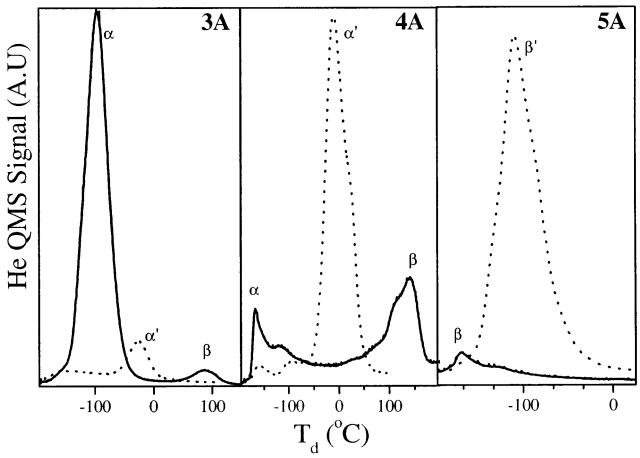

Figure 1. Temperature-programmed He decapsulation curves (20 °C/min) from dried (solid) and wetted (doted) 3A, 4A, and 5A zeolites. Bare and tagged Greek letters denote decapsulation peak assignments in the dry and wet states, respectively. All presented curves are equally scaled.

members of type-A zeolites. Samples of as purchased *hydrated* grades, each weighing ca. 300 mg, were used. The grades used were 1/16" 3A and 4A pellets, and 8−12 mesh 5A spheres, manufactured by BDH, Sigma, and J. T. Baker Chemical Co., respectively. Dehydration of samples was performed at various temperatures (T_w), for 30 min under active vacuum. For each dehydration treatment at a given temperature, two identical sorption procedures were performed for He and Ne. Sorption was carried out in a *dynamic* fashion, by flowing the gas over the sample during cooling between T_w and liquid nitrogen (LN_2). Sorption was accomplished with a prolonged evacuation of excess gas at LN_2, after which inert carrier gas was introduced (He was used for Ne desorption measurements and vice versa). TPD_c was performed by linearly (20 °C/min) heating the sample from LN_2 to just about T_w. Successive sorption of the other gas was then carried out from T_w down to LN_2. After each set of He and Ne measurements, the sample was heated to a higher T_w that was utilized for the next set of sorption/TPD_c measurements. In that way, TPD_c measurements were taken separately for each grade, and for He and Ne, versus T_w along the (RT, 400 °C) temperature range.

Results and Discussion

Figure 1 illustrates the strong effect that water content has on the decapsulation phenomenon from the various type-A zeolites. For each grade, representative TPD_c profiles are shown for the two extreme states of dehydration, i.e., for dry and wet substances (solid and dotted curves, respectively). For clarity, only He decapsulation profiles are shown due to their better resolution with respect to those of Ne, for which qualitatively the same behavior was observed. It is worth mentioning that all the TPD_c profiles presented in Figure 1 are background (blank TPD reactor) subtracted.

The characteristic common structure of the TPD_c profiles is first discussed by considering those acquired for the dry grades. In general, depending on zeolite grade, the TPD_c profiles are seen to consist of up to two principal decapsulation peaks. The low-T peaks, centered around −170 °C in the cases of dehydrated 4A and 5A, were previously attributed to α and β encapsulations, respectively.[1,8] These low-T peaks however, depict poor encapsulations in the sense that the closure of the O_6 windows of the β cage, and certainly of the wider O_8 windows of the α cages, in 5A and 4A, respectively, is ineffective for an efficient quantitative entrapment of Ne and moreover for He, even at temperature as low as LN_2. Upon evacuation of dried 4A and 5A samples at LN_2, most of the pre-admitted gas slowly discharges, strongly indicating the imperfect enclosure of the relevant apertures in these grades.[1]

In contrast to the above, the closure of α apertures in 3A to He and Ne is seen to be practically perfect at LN_2, and this closure probably remains practically tight even at somewhat higher T. The low-temperature decapsulation peaks of He in 3A thus exceed −170 °C, shifting toward a higher temperature of ca. −100 °C. In principle, due to the growing diameter of the neutralizing cations occurring on passing from 5A to 3A via 4A, one expects that practical permeability to 5, 4, and 3A would, respectively, require larger dilation, i.e., higher temperatures. Indeed, a higher temperature is required to sufficiently dilate the O_8 windows of the α cavities in 3A in order to provide efficient penetration for He and Ne. This is clearly evident from a rough comparison between peaks locations in dried samples. In Figure 1, the decapsulation temperatures of 3A show up at higher temperatures with respect to 4A, shifting for He from ∼ −170 °C in 4A toward ∼ −100 °C in 3A, and more pronouncedly in the case of Ne,[1] from ∼ −170 °C to about 50 °C, respectively. In 5A, apart from the low-temperature decapsulation peak, the absence of any additional peaks at higher temperatures is clearly understood as occurring due to the large aperture openings of this grade. The occurrence of a second He decapsulation peak in 4A, at high temperature near 150 °C, was assigned in ref 1 to β encapsulation. Similarly, the two peaks observed for He/3A, i.e., at −100 and ∼90 °C, were assigned to decapsulations from the α and β cages, respectively.[1] An identical qualitative behavior of the decapsulation profiles was practically observed for the case of Ne, however, with decapsulation peaks that are shifted toward higher temperatures with respect to He, as expected for the larger Ne atom.[1] Finally, it should be mentioned that the curves of Figure 1 were cut off, for clarity, at decapsulation temperature values (T_d) beyond which no additional peaks, other than those presented, were observed (up to 400 °C) for either dried or wetted samples.

Close examination of the TPD_c profiles of Figure 1 reveals clear essential differences between dried and wetted grades. TPD_c peaks in the wetted states (dotted curves in Figure 1) shift toward higher decapsulation temperatures with respect to those recorded for dried samples. Such a shift implies a more efficient aperture closure. It may also be noted in Figure 1 that the shifts of the α and β TPD_c peaks in 4A and 5A, respectively, are accompanied with growing intensities, i.e., larger encapsulation capacities are achieved for these particular cages in the wetted state. A clear dissimilarity, however, is evident for the β cages of 3A, where increment of water content suppresses encapsulation by these cages. Such a behavior may be viewed as a clear indication for the blocking effect of water molecules. In dry 4A and 5A, where the free aperture dimension of the O_8 and O_6 windows, respectively, is sufficiently large and encapsulation is rather poor, addition of water molecules causes an effective closure of theses windows, i.e., a reduction in their free dimension, to an extent of optimal entrapment by these cages. As a result, the encapsulated amounts strongly grow in the wetted state. On the contrary, in dry 3A whose both kinds of apertures are already closed to a larger extent with respect to 4A and 5A, hydration increases the effective blocking of the O_6 and O_8 apertures to extents of reduced α encapsulation and of completely suppressed β encapsulation (under the sorption conditions used here). For different intermediate states of dryness, the recorded TPD_c curves of He and Ne from the

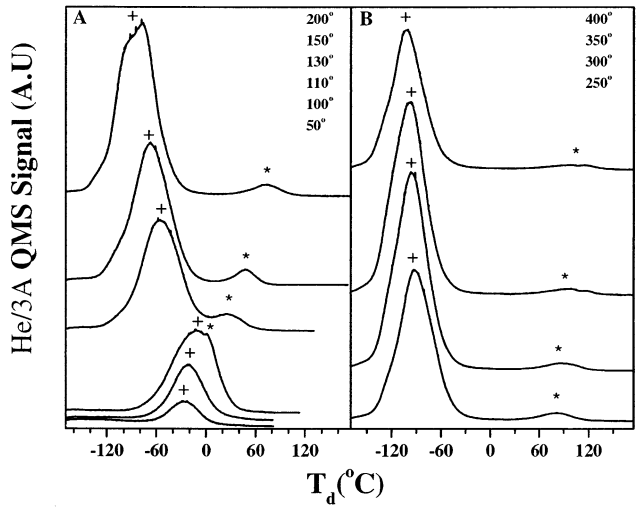

Figure 2. Evolution of temperature-programmed decapsulation curves of He from 3A versus dehydration temperatures. Dehydration temperatures (in centigrade units) are depicted in accordance with the order of curves appearance. Crosses and asterisks lead the eye through the shift effect of the α and β decapsulation peaks, respectively.

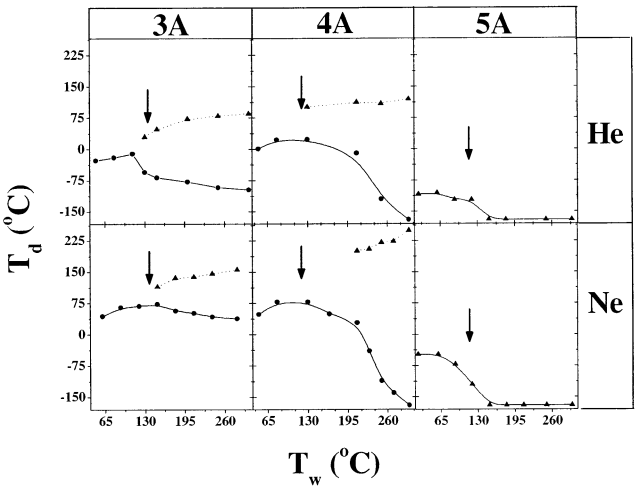

Figure 3. Dehydration curves (decapsulation temperatures vs dehydration temperatures) of He and Ne from 3A, 4A, and 5A zeolites. Circles and triangles represent α and β decapsulations, respectively. Dotted and solid lines were passed through data points to lead the eye. Arrows represent maximal desorption rates of water molecules from the various grades, as measured by performing TPD between RT and 300 °C on hydrated *unloaded* samples.

various grades practically possessed similar peak structure, however, with varying peak shifts and intensities. Representative accumulated data are shown in Figure 2 for the case of He/3A. In the wetted form (lower curve in Figure 2A), a single small He decapsulation peak is seen to occur around −30 °C. Upon dehydration at T_w = 100 °C, the TPD_c curve remains single peaked, however with a larger intensity and a small shift toward higher decapsulation temperature of ca. −20 °C. Dehydration at 110 °C results in a further higher decapsulation peak (∼ −10 °C), as well as in an interesting building up of a double peaked hump, indicating the initiation of splitting. From that T_w on, as the dehydration temperature is raised and the water content of the zeolite decreases, the split is enhanced with improved resolution and with a growing temperature gap between its two constituent peaks, such that the high temperature peak shifts toward higher decapsulation temperatures while the low temperature component shifts toward lower decapsulation temperatures. The crosses and asterisks in Figure 2 follow up this interesting trend whose overall behavior was found to be common to all grades and gases used in the present work. The overall data accumulated from typical decapsulation experiments, taken for various T_w ranging between RT and 300 °C, is summarized in Figure 3. The resultant curves of decapsulation temperatures, T_d, versus those of dehydration, T_w, are hereby referred to as "dehydration" curves. The lines passing through the data points of Figure 3, lead the eye throughout the shape of the dehydration curves. The exact partition to upper (dotted) and lower (solid) curves is rather speculative as subjugated to the suggested interpretation discussed below.

Structurally, the shapes of the 3A and 4A dehydration curves practically resemble a double tooth fork with the following common features: (i) the fork's handle evolves monotonically with T_w toward higher T_d up to its node, where splitting occurs. This part of the fork depicts the shift of the initial single decapsulation peak of the wetted state toward higher decapsulation temperatures upon mild dehydration. This trend is accompanied by relatively steep growing of decapsulation amounts (not shown graphically). (ii) Splitting is observed only in 3A and 4A zeolites. In 3A, splitting is distributed rather narrowly around an average critical dehydration temperature T_{wc} of about 120 °C, and is rather continuous with respect to T_d. In 4A, the situation is less obvious due to the T_d-discontinuity of the He and Ne dehydration curves. Nonetheless, in view of another clue observation discussed below, one may speculate that splitting in the case of 4A occurs also around the same T_{wc} ∼ 120 °C measured for 3A. (iii) The two resulting branches evolve versus T_w in a systematic symmetric fashion. In the lower branches, T_d decreases with T_w, whereas the upper ones evolve with growing T_d values. (iv) A comparison between the fully dehydrated forms of 4A and 3A (those data points corresponding to the highest T_w values) reveals that the lower and higher branches of 4A have, respectively, noticeable lower and higher T_d values with respect to 3A. (v) The single-branched dehydration curves of 5A imply the occurrence of only one class of decapsulation site for both He and Ne.

According to the above peaks ascriptions, the lower and upper branches of the 3A and 4A dehydration curves (Figure 3) are assigned to α and β decapsulations, respectively. In the case of 5A, its sole branch is assigned to β decapsulation. This is supported by the fact that all Ca atoms in 5A are known to lie near the center of 6-rings.[17]

The first observation to be resolved is the branching phenomenon, i.e., the occurrence of a critical dehydration temperature in 3A and 4A, seeming to occur with a common T_{wc} value, irrespective of grade and gas types. A possible origin for such a "global" T_{wc} value was traced out by recording the signal of water (m/z = 18) desorbing upon dehydration of fully hydrated type A samples (*unloaded* with He or Ne) along the (RT, 350 °C) temperature range. The TPD spectra of water desorbing from those wetted 3A, 4A, and 5A, were similarly structured, composed of a single broad water desorption peak centered at about 135, 117, and 115 °C, respectively (indicated by arrows in Figure 3). At these temperatures, the rates of water desorption (dehydration) are maximal. Most interestingly, this rather narrow distribution of temperatures perfectly meets that of T_{wc} value measured for 3A, thus supporting the above speculation of an identical T_{wc} value for the 4A grade. The above clue observation implies the occurrence of a firm relation between the zeolitic water content and apertures free dimension, and is accordingly utilized for the interpretation of the common behavior of the dehydration curves of Figure 3. From a close

inspection of Figure 3, it may be fairly agreed that in 3A and 4A, T_d increases with T_w up to the vicinity of T_{wc} at which the dehydration rate is maximal, indicating a tendency of slight effective aperture closure along this dehydration temperature range. Beyond the branching point, the upper branch inclines with T_w, while the lower one responds with declining T_d values. The above observations are understood by combining structural and ion relocations considerations. The increasing vacancies are those that ultimately induce ion relocations from which the final state of cation distribution is derived. This, in turn, dictates the extent of windows blocking as hereby explained. The inherent structure of cages in A-zeolites is such that the β cavities are interlinked via α ones, thus gas diffusing from one β cavity to the next must go through a connecting α cage. α cages however, are directly interlinked. As a result, β decapsulation must *always* occur after that from α cages, i.e., encapsulated gas must first be discharged from α cages. The fork's handle in Figure 1 thus depicts decapsulation from α cages. The mild effective enclosure of the above O_8 apertures, seen to occur at the early stages of dehydration, is interpreted as follows. In the fully hydrated state, where the sample is saturated with water molecules, the zeolitic cages (both α and β) are mostly occupied by water molecules. The water content at this stage is sufficiently large, dimensionally restricting encapsulation, mainly in β cages. At the beginning of dehydration, water is removed from the inner volume of the α cage and the emptying volume progressively becomes available for encapsulation. In the course of dehydration, the possibility of the counterions to stack near or in the windows increases.[2,9] Under these conditions, the average blocking of O_8 windows slightly increases, a trend which is clearly observed by the occurrence of increment T_d values in 3A and 4A upon mild dehydration. During this initial stage of dehydration, water content is still sufficiently large, leaving the smaller O_6 windows of β cages practically closed. This situation dominates upon increment of evacuation temperature, however only up to the point at which dehydration becomes harsh and the rate of water loss increases gradually. At that point the dehydration curve splits: O_6 windows begin to unlock and β cages become available for encapsulation. The vacant β cages expose the counterions to their stronger bonding energies,[4,5] causing them to relocate at these energetically favorable sites. This ultimately causes the counterions to strand to growing extents at channels intersections or on channel walls associated with the O_6 windows, which consequently take up the majority of counterions blocking effect. As a result, the admission of He and Ne into the β cages is seriously inhibited, whereas O_8 apertures are left more vacant. The above interpretation explains the observed splitting phenomena as well as the reversing of the blocking state of the O_8 windows taking place at T_{wc}. Admission of a given atom into α cages is thus relatively eased, while admission into β cages becomes arduous. Eventually, due to the above, inclining β- and declining α-branches are observed in the 3A and 4A.

Another possible mechanism which could govern inclining β- and declining α-branches in 3A and 4A is suggested by referring to a possible indirect effect that heating may have on lattice readjustments. Apart from cations, the framework channels[9] may also contain hydroxyl groups. The common major TPD peak of water occurring around 120 °C could also be due to thermal decomposition of OH groups. The occurrence of such hydroxyl groups was observed in 5A,[17−20] and reported also for 4A;[21] however, it was not tested for the case of 3A. By considering the existence of such OH groups in type-A zeolites, an alternative interpretation of the post branching part of the dehydration curves is suggested. It is known for other substances that while evacuation up to about 120 °C mainly removes physisorbed water molecules,[10] at that temperature and above hydroxyl groups are also removed as water.[10,11] If the hydroxyls in the case of A-zeolites occur at the channels running across the framework, their removal may effectively result in constricted channels (i.e., partial collapse). Such a situation was reported for some zeolites of narrow channel networks where adjustments upon dehydration took place.[9] The present observation of a common branching temperature around 120 °C could thus be in accordance with the above, and the inclining behavior of the β branches may be understood as a direct expression of a sintering-like effect occurring due to such partially collapsed channels. Since O_8 apertures are much wider than those of the smaller O_6 windows, α encapsulation seems insensitive to the above speculated constriction effect.

The systematic occurrence of higher β-T_d values in 4A compared to those in 3A, depicts an apparent inconsistency with respect to the fundamental dimensional considerations on which the encapsulation mechanism relies. This is because in comparison to 4A, 3A contains larger sentinel K^+ ions, and its β apertures are thus expected to undergo a much more firm blocking. One would thus expect gas admission to β cages in 3A to occur at higher temperatures relative to those required in the case of the apparently "less blocked" 4A$-O_6$ apertures. While this expectation is indeed fulfilled in the case of α encapsulation involving the larger O_8 windows, it is evidently violated in the case of β encapsulation. For example, He (Ne) decapsulates from β cages in 3A at $\sim$ 90 °C (160 °C), while in 4A this occurs only at $\sim$120 (250 °C). The "reversed size effect" results from the fact that in A-zeolites larger univalent cations of diameters above ca. 1 Å (such as K^+ in 3A) relocate in the zeolitic framework in such a way that a weaker blocking effect on O_6 windows is achieved as compared with smaller counterions such as Na^+.[8,12]

Interestingly, although only β encapsulation is manifested in 5A, the dehydration curve of 5A has a behavior similar to those of the 3A and 4A α branches. Moreover, Figure 3 shows that the dehydration curve of 5A (for both He and Ne) evolves versus T_w with T_d values that are lower even than those of the 3A and 4A α branches. This means that despite the presence of water molecules, their net closure effect on the O_8 windows in 5A is very small, even at LN_2. This may be understood by accounting for the divalent nature of the Ca^{2+} cations that makes their critical diameter significantly smaller than those of the univalent ones, and moreover, due to their divalent nature they are presented in half the number K^+ and Na^+ do. Soon, a complementary ambient encapsulation study will be carried out by using larger atoms such as Ar, and Xe that might manifest α encapsulation at low temperature also in 5A.

A final remark concerns the direct effect of temperature on the free aperture dimension of the zeolitic windows.[1,8] This effect was ignored throughout the present discussion due to its obvious trend on both O_6 and O_8 windows in either zeolite grade, i.e., both dilate and contract upon heating and cooling, respectively.[1,8,13−16] The net effect of thermal dilation/contraction is nicely observed in the dehydrated state as discussed in detail in ref 1. By ignoring here such effect acting in the same direction on either kind of windows, the generality of the present discussion is not affected. In view of the above, the qualitatively unambiguous opposed behaviors observed here for the α and β branches of the dehydration curves only reinforce the suggested role taken by ion relocations due to removal of water molecules.

Conclusions

Water content was shown to be a valuable tool for probing the roles played by different mechanisms that determine the effective apertures dimension in A zeolites. The use of inert atomic encapsulate probes enabled the extraction of pure dimensional effects. The results indicate the occurrence of a subtle balance between several mechanisms, including relocations of counterions and possible lattice adjustments. The observed decapsulation behavior was shown to be fully consistent with the characteristic sizes of the atomic probes and of the apertures offered by the various zeolite grades. It is concluded that the net effect of dehydration is to preferably open the O_8 windows, while reducing the opening of the smaller O_6 apertures. The above result may be viewed as an experimental realization of longstanding speculations as for the ability of zeolites to undergo significant lattice adjustments upon dehydration/rehydration.

References and Notes

(1) Finkelstein, Y.; Saig, A.; Danon, A.; Koresh, J. E. *J. Phys. Chem B* **2003**, *107*, 9170.

(2) Breck, D. W. In *Zeolite Molecular Sieves*; Wiley: New York, 1974.

(3) Barrer, R. M. In *Zeolites and Clay Minerals as Sorbents and Molecular Sieves*; Academic Press: New York, 1978.

(4) Qiu, P.; Huang, Y.; Secco, R. A.; Balog, P. S. *Solid State Ionics* **1999**, *118*, 281.

(5) Stamires, D. N. *J. Chem. Phys*. **1962**, *36*, 3174.

(6) Szynaski, H. A.; Stamires, D. N.; Lynch, G. R. *J. Opt. Soc. Am.* **1960**, *50*, 1323.

(7) Rabinowitch, E.; Wood, W. C. *Z. Elekrtochem*. **1933**, *39*, 562; Taylor, W. H. *Proc. R. Soc*. **1934**, *A145*, 80; Beattie, I. E.; Dryer, A. *Trans. Faraday Soc*. **1957**, *53*, 61.

(8) Saig, A.; Danon, A.; Finkelstein, Y.; Koresh, J. E. *J. Chem. Phys*. **2003**, *118*, 4421.

(9) Barrer, R. M.; Vaughan, D. E. W. *Trans. Faraday Soc.* **1971**, *67*, 2129.

(10) Danon, A.; Avraham, I.; Koresh, J. E. *Rev. Sci. Instrum.* **1997**, *68*, 4359.

(11) *The Age of the Molecule*; Hall, Nina, Ed.; Royal Society of Chemistry, 1999.

(12) Fraenkel, D. *J. Chem. Soc., Faraday Trans. 1* **1981**, *77*, 2041.

(13) Jobic, H.; Bee, M.; Pouget, S. *J. Phys. Chem. B* **2000**, *104*, 7130.

(14) Kopelevic, D. I; Chang, H. C. *J. Chem. Phys*. **2001**, *115*, 9519.

(15) Deem, M. W.; Newsman, J. M.; Creighton, J. A. *J. Am. Phys. Soc*. **1992**, *114*, 7198.

(16) Kirk-Othmer, *Encyclopedia of Chemical Technology*, 3rd ed.; Wiley: New York, 1981; pp 115, 647.

(17) Pluthand J. J.; Smith, J. V. *J. Am. Chem. Soc.* **1983**, *105*, 1192.

(18) Corbin, D. R.; Farlee, R. D.; Stucky, G. D. *Inorg. Chem.* **1984**, *23*, 2920.

(19) Mix, H.; Pfeifer, H.; Staudte, B. *Chem. Phys. Lett.* **1988**, *146*, 541.

(20) Paoli, H.; Bataillc, T.; Rebours, B.; Methivier, A.; Jobic, H. *Stud. Surf. Sci. Catal.* **2001**, *135*, 2870.

(21) Pruski, M.; Ernst, H.; Pfeifer, H.; Staudte, B. *Chem. Phys. Lett.* **1985**, *119*, 412.